ISSN (Online) 2394-6849
International Journal of Engineering Research in Electronics and Communication Engineering (IJERECE)
Volume 12, Issue 03, March 2025

Advanced FPGA-Based System for Real-Time Detection of Respiratory Leakage in Fit Testing Clinics

[1] Niranjankumar K, [2] Sivaramireddy M, [3] Lokesh V, [4] Madhavan P
[1] [2] [3] [4] Department of ECE, Muthayammal Engineering College, Namakkal, Tamil Nadu, India
Corresponding Author Email: [1] nk880040@gmail.com, [2] reddysivaram46@gmail.com, [3] Lokesh.varikallu01112003@gmail.com, [4] madhavanecevlsi@gmail.com

Abstract— A portable system for rapid wheezing detection is proposed, designed for long-term patient monitoring and potential integration with other biomedical signal systems. The system utilizes a field-programmable gate array (FPGA) to accelerate the detection process. Sound signals are segmented into 2-second units and analyzed using a short-time Fourier transform to create spectrograms. These spectrograms are then processed using a series of techniques including 2D bilateral filtering, edge detection, multi-threshold image segmentation, morphological image processing, and image labeling. This processing extracts wheezing features based on computerized respiratory sound analysis (CORSA) standards. These features are used to train a support vector machine (SVM) for wheezing classification. The system is implemented on a Xilinx Virtex-6 FPGA ML605 platform. Testing demonstrates a wheezing recognition performance of 0.912, with the detection process operating at a clock frequency of 51.97 MHz, enabling rapid classification.

Index Terms: rapid wheezing detection, field-programmable gate array (FPGA), spectrogram image processing, support vector machine (SVM).

I. INTRODUCTION

Asthma and chronic obstructive pulmonary disease (COPD) are prevalent, with environmental factors like air pollution contributing to their rise. Analyzing respiratory sounds, particularly wheezing, can provide valuable diagnostic information about lung health. Current diagnostic methods for asthma include auscultation, spirometry, and peak expiratory flow measurement. Auscultation is subjective, while spirometry can be uncomfortable and unsuitable for continuous monitoring. Analyzing recorded lung sounds via signal processing offers a more objective approach to identifying abnormal characteristics and understanding the underlying physiological mechanisms. Asthma is a chronic disease with a risk of life-threatening acute attacks. Effective long-term management is crucial, but many patients discontinue treatment, leading to declining lung function. A portable, rapid wheezing detection system is needed for timely warnings and home care. Wheezes are abnormal respiratory sounds characterized by specific frequency (above 100 Hz) and duration (over 100 ms). Spectrograms are commonly used for wheeze analysis, but are susceptible to noise. Existing wheezing feature extraction methods include combining classification models with algorithms (computationally intensive) and image processing of spectrogram edges (resolution-dependent). The computational demands of accurate wheezing detection often restrict traditional systems to desktop computers. Portable systems using DSPs may be limited by sequential processing, while custom ICs are inflexible and expensive. Our wheezing recognition system, illustrated in Figure 1, comprises three stages: 1. Preprocessing: A short-time Fourier transform (STFT) generates a spectrogram representing the time-frequency characteristics of the wheezing sound. 2.Spectrogram Masking: Bilateral filtering reduces noise while preserving edges. Subsequent image processing techniques (edge detection, multi-threshold segmentation, and morphological processing) identify potential wheezing regions. These regions are then validated against two CORSA-based rules to ensure they represent actual wheezes. 3.Feature Extraction and Classification: Features representing the wheezing components within the masked spectrogram are extracted and classified using a Support Vector Machine (SVM). Spectrogram image processing is central to this system. Unlike traditional methods that directly analyze spectrogram edges or solely rely on peak continuity rules after filtering, our approach combines these strategies. Bilateral filtering smooths the image while preserving prominent edges. The combination of edge detection and multi-threshold segmentation maintains both edge integrity and distinct peaks for analysis.

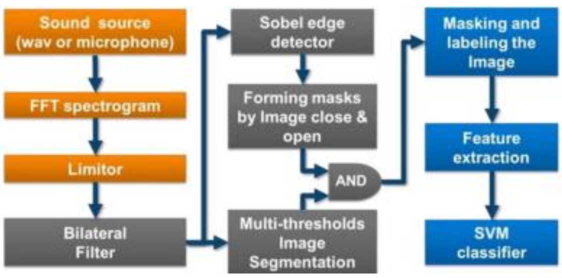

Figure 1. Wheeze detection algorithm processing flow

ISSN (Online) 2394-6849

International Journal of Engineering Research in Electronics and Communication Engineering (IJERECE)

Volume 12, Issue 03, March 2025

1.1. SoPC Hardware Architecture:

The proposed wheezing detection system was implemented as an independent Wheezing Detection System IP (WDSIP). Following a System-on-a-Programmable-Chip (SoPC) design flow, the WDSIP can be integrated with other subsystems on a single FPGA, enabling efficient on-chip data transfer and reducing I/O requirements and external IC usage. This design allows for both standalone operation and integration within a larger physiological parameter measurement system. Using Xilinx's Embedded Development Kit (EDK), a MicroBlaze soft processor was embedded within the WDSIP, as shown in Figure 2. This enables communication with other hardware IPs via the Processor Local Bus (PLB). Provided the WDSIP's timing adheres to the PLB communication protocol, the MicroBlaze can control register settings within the memory map.

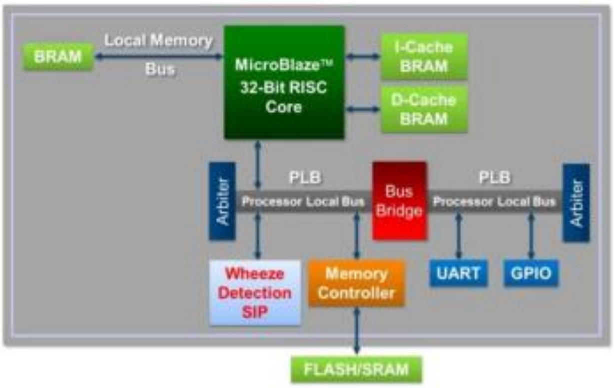

Figure 2. Integrated WDSIP with MicroBlaze processor

1.2. Proposed Wheezing Sound Detection System

The WDSIP is designed for PLB communication with other cores. Given the extensive read/write operations involved in bilateral filtering and image mask generation (Figure 1), on-chip memory within the WDSIP stores intermediate data. This minimizes PLB bandwidth usage and improves processing speed. The WDSIP utilizes a single PLB slave interface. The MicroBlaze processor's role is limited to writing sound data to the WDSIP and reading the final classification result from a control register in the memory map.

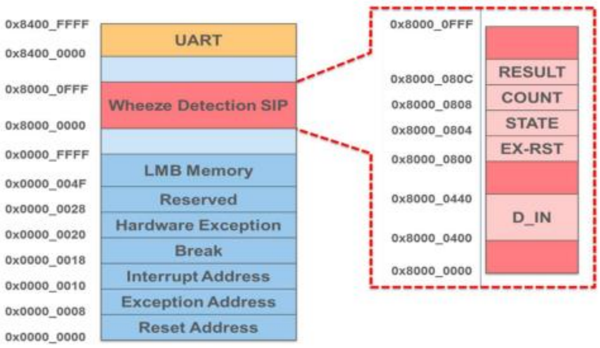

Figure 3. Memory management.

Table 1. WDSIP internal register.

Register Name	Direction	Description
EX_RST	I	Reset the wheezes detection SIP.
D_IN	I	Input raw data of breath sound.
STATE	O	Current processing state for MicroBlaze monitoring.
COUNT	O	Counting current input data for MicroBlaze processing bit-error check.
RESULT	I/O	Detection result register, which will be cleared by MicroBlaze when the result has been read.

II. DESIGN OF WDSIP

Wheezing sounds are characterized by a fundamental frequency and its harmonics. Visually, these appear as nearhorizontal lines on a spectrogram, indicating a dominant frequency sustained over time. Our WDSIP is designed for rapid identification of these wheezing patterns by distinguishing their edges from background noise within the spectrogram. The key components of the WDSIP are described below.

2.1. STFT Implementation

Once the WDSIP receives a frame of audio data, the FSM proceeds to the STFT stage. A 256-deep dual-port RAM, configured in read-after-write mode, temporarily stores the data. This allows the newly stored data to be available at the output port after a single clock cycle. This data is then multiplied by a Hanning window to generate the first data frame. The RAM's other port waits 128 cycles before reading the next 128 data points to compute the subsequent frame. This process repeats to implement a 50% overlapping Hanning window. Figure 8 illustrates the hardware implementation of this windowing process.

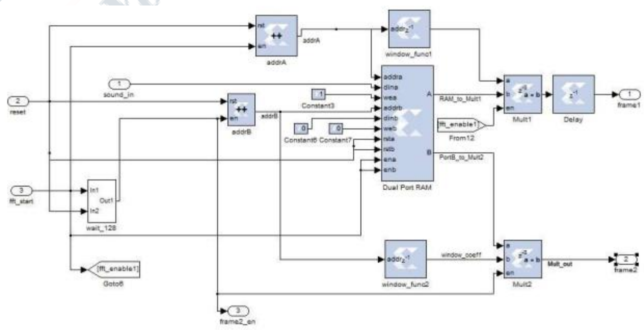

Figure 4. Implementation of 50% overlapping Hanning window.

2.2. Implementation of the Bilateral Filter

Our WDSIP's bilateral filter implementation is based on the method described in [26]. A 7x7 filter mask is implemented in hardware. Calculating a single filtered pixel requires computing 49 weights and multiplying them by the corresponding neighboring pixels. To avoid excessive computation and reliance on external memory, a line buffer and register matrix are used to implement the filter mask. This enables continuous image processing, with a new pixel processed at each clock cycle. The image mask shifts

ISSN (Online) 2394-6849
International Journal of Engineering Research in Electronics and Communication Engineering (IJERECE)
Volume 12, Issue 03, March 2025

horizontally with each pixel clock, ensuring all necessary neighborhood values are available for weight calculation. A filtered central pixel is thus generated at every pixel clock, a speed not readily achievable on a standard desktop PC. Figure 9's timing diagram illustrates the delay line-based hardware implementation for populating the filter window.

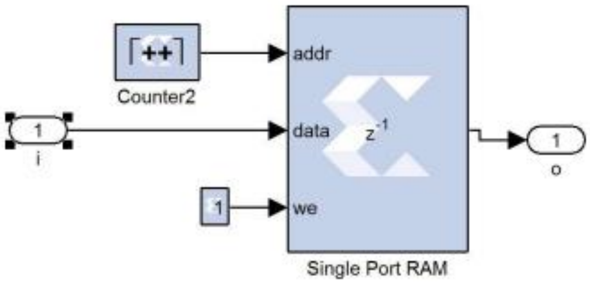

Figure 5. Implementation of the line buffer.

2.3. Implementation of Multithreshold Image Segmentation

Multi-threshold segmentation involves applying a threshold to the filtered spectrogram, labeling resulting image objects, and isolating them based on defined rules. The hardware implementation of the labeling system. Initially, a class register array is cleared and initialized. Two pixels (P1 and P2) from the thresholded image are read and assigned to a label block for temporary labeling. These labeled pixels are then sent to both temporary image memory and delay lines for moving window implementation and connectivity checking. Because the labeling block may generate two equivalent pairs concurrently, and the class register updates serially, a combining block processes these pairs, ensuring they are sent one at a time. Finally, the temporary images are read from memory and connected based on the class register array's contents. Isolating wheezing components through multi-threshold image segmentation, which may require multiple iterations with varying thresholds and object characteristic analysis, is the most time-intensive process in the WDSIP. To optimize speed and resource utilization, dual-port RAM and pipelining are applied to the image labeling system for maximum clock rate and throughput. However, due to the simultaneous use of one RAM port for bilateral filter output, that port's operational frequency is limited. To address this, a time-division demultiplexer concurrently sends two pixels to the labeling block, and a time-division multiplexer combines the labeling system's output. This maintains the maximum pixel processing rate while halving the timing constraints within the labeling system.

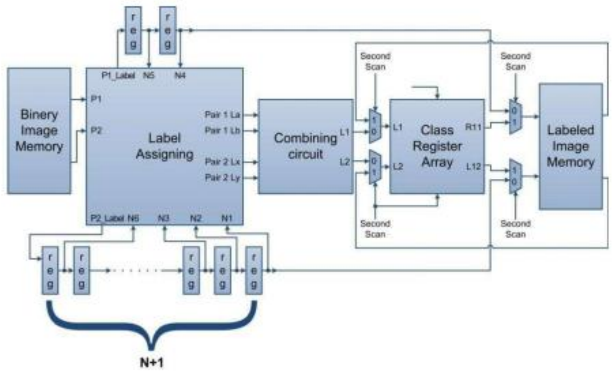

Figure 6. Hardware architecture of image labeling.

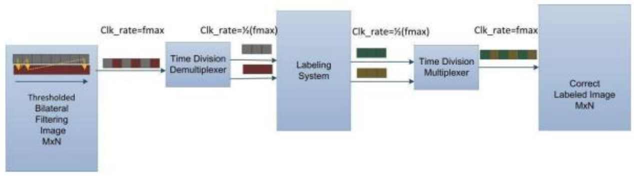

Figure 7. Modified raster scan for labeling system.

2.4. Implementation of Wheezing Mask Formation

While multi-threshold segmentation identifies numerous objects meeting CORSA criteria, not all are actual wheezes. Therefore, edge detection is used to identify quasi-horizontal lines with significant gradients. Combining the results of multi-threshold segmentation and edge detection creates a mask, isolating objects with both high intensity and distinct edges, which are then classified as wheezing components. Figure 13 shows the hardware implementation of the Prewitt edge detection operator.

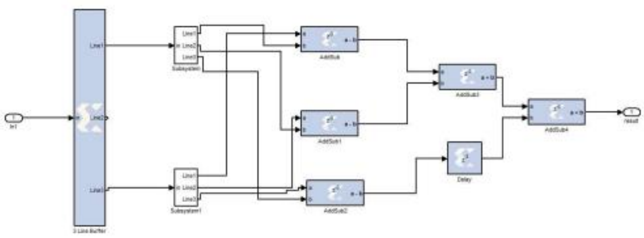

Figure 8. Edge detection processing elements.

III. RESULTS AND DISCUSSION

3.1. Wheezing Sound Detection Results

An SVM classifier was used to distinguish wheezing from normal sounds based on the properties of the spectrogram objects identified by the mask. Four parameters were chosen as wheezing features

1. PCY: Centroid frequency of the wheezing episode.
2. PT: Duration of the wheezing episode.
3. PS: Slope of the wheezing episode.
4. PAR: Ratio of the wheezing episode area to its bounding box area.

ISSN (Online) 2394-6849

International Journal of Engineering Research in Electronics and Communication Engineering (IJERECE)

Volume 12, Issue 03, March 2025

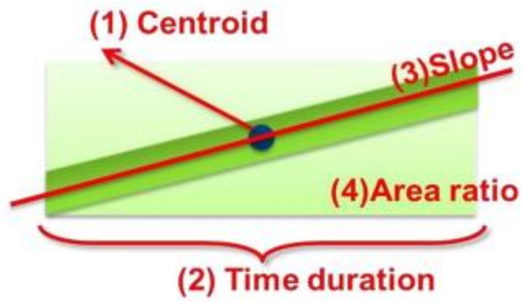

Figure 9 Parameter for extracting wheezing features.

The SVM classifier requires prior training. An RBF kernel and grid search were used to optimize the σ parameter for optimal performance. Figure 15 shows the wheezing recognition accuracy achieved with different SVM parameter sets. This analysis validated the chosen parameters' effectiveness in representing wheezing features and identified the most efficient parameter combination. Breath sound recordings from National Taiwan University Hospital [27] were used, divided into training (11 asthmatic patients, 10 healthy individuals) and testing (13 asthmatic patients, 12 healthy individuals) sets. All sound files were segmented into 2-second units.

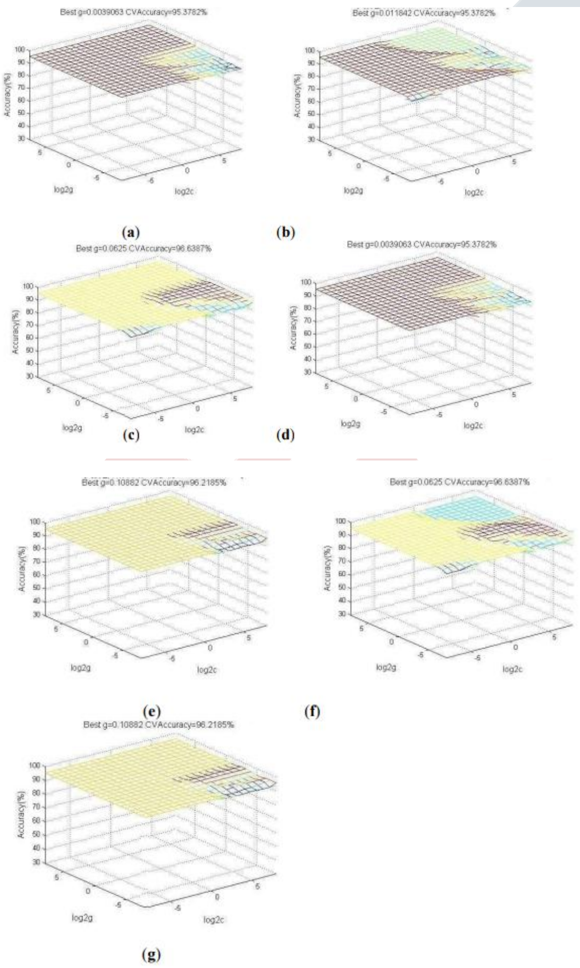

Figure 10 (a, b, c, d, e, f, g)

Figure 11 (a) Grid searching (Features: PT, PCY); (b) Grid searching (Features: PT, PAR); (c) Grid searching (Features: PT, PS); (d) Grid searching (Features: PT, PCY, PAR); (e) Grid searching (Features: PT, PCY, PS); (f) Grid searching (Features: PT, PAR, PS); (g) Grid searching (Features: PT, PCY, PAR, PS)

Training results showed the system achieved up to 96.63% accuracy using feature sets (PT, PS) and (PT, PAR, PS). The trained SVM models were then used to classify the testing data. System performance was evaluated by calculating sensitivity (SE) and specificity (SP).

$$Sensitivity = \frac{True\ Positive\ TP\ (\ \ )}{} \quad (1)$$

$$Specificity = True\ +Positive = Fasle\ \sqrt{Sensitivity True\ Positive(FP)(TP\ Negative(TN)) + Fasle} \times Specificity\ Negative\ \frac{}{(FN)}$$

$$(2)\ True\ Negative(TN) Performance \quad (3)$$

TAnalysis of the testing samples with various parameter sets showed the best performance with (PT, PS) and (PT, PAR, PS). The (PT, PS) set was chosen for hardware implementation due to its lower resource requirements. Figures 16 and 17 show the results of this hardware-implemented SVM. Wheezing is detected when the SVM output exceeds 26. To verify the WDSIP's wheezing detection performance after hardware implementation, the same testing samples were sent to the platform via the UART port. Tera Term, with a serial port band rate of 115,200 bps, was used for connection to the platform to assess UART transmission reliability. A data set (0-232) was written. to a file, and sent this file to the platform, where a program we had written compared the received data with an accumulator, the estimated error rate of UART transmission was obtained. The results show that no errors were observed when these 4,294,967,296 testing samples were sent to the platform. As previously mentioned, fixed-point hardware operations allow for prediction of wheezing recognition error. To estimate this error, hardware results were compared against the assumed-correct software results. The primary source of discrepancy is the LUT depth used for storing photometric filter weights. Weight coefficient quantization, with 8192 stored coefficients and a precision limited to 0.01, introduces quantization error. This error reduces the signal-to-noise ratio (SNR) of the wheezing signal, impacting system performance.

IFERP Explore Your Research Journey...
ISSN (Online) 2394-6849
International Journal of Engineering Research in Electronics and Communication Engineering (IJERECE)
Volume 12, Issue 03, March 2025

Table 2. Recognition results for different features.

Selected Features	TP	TN	FP	FN	Sensitivity	Specificity	Performance
(P_T, P_{CV})	128	209	21	13	0.907801	0.908696	0.908248
(P_T, P_{AR})	128	209	21	13	0.907801	0.908696	0.908248
(P_T, P_S)	128	215	15	13	0.907801	0.934783	0.921193
(P_T, P_{CV}, P_{AR})	128	209	21	13	0.907801	0.908696	0.908248
(P_T, P_{CV}, P_S)	124	221	9	17	0.879433	0.96087	0.91925
(P_T, P_{AR}, P_S)	128	215	15	13	0.907801	0.934783	0.921193
(P_T, P_{CV}, P_{AR}, P_S)	124	221	9	17	0.879433	0.96087	0.91925

Table 3. Recognition results from Matlab and hardware.

	TP	TN	FP	FN	Sensitivity	Specificity	Performance
Matlab	128	215	15	13	0.907801	0.934783	0.921193
Hardware	125	216	14	16	0.88652482	0.93913043	0.9124486

Table 3 shows that hardware performance is affected by quantization error. This error significantly impacts wheezing detection, which relies on gradient estimation via first-derivative calculations. Increasing LUT size for higher precision is a potential solution, but it increases hardware resource demands. Therefore, a new SVM model was trained using features directly extracted from the hardware, allowing the SVM to compensate for the quantization effects.

3.2. Implementation Results of the WDSIP

The WDSIP was implemented using a Xilinx Virtex-6 FPGA ML605 platform. The internal placement and routing of the FPGA is illustrated in Figure 11. The total hardware resources used by the WDSIP are listed in Table 4 and Figure 12

Table 4. A summary of the resource usage by WDSIP.

	Spectrogram	Bilateral Filtering	Image Labeling System	Morphological Processing	Total Used
Slice Register	17511	12881	9228	6449	46069
Occupied Slices	4095	3783	3436	3073	14387
Block RAMs	62	69	48	20	199
DSP Slices	57	66	55	14	192

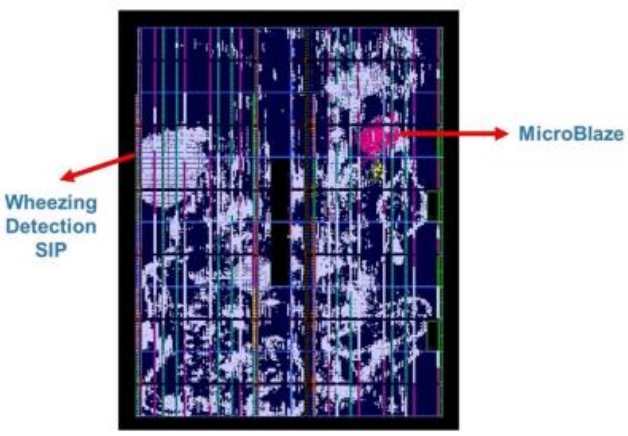

Figure 12. FPGA internal placement and routing

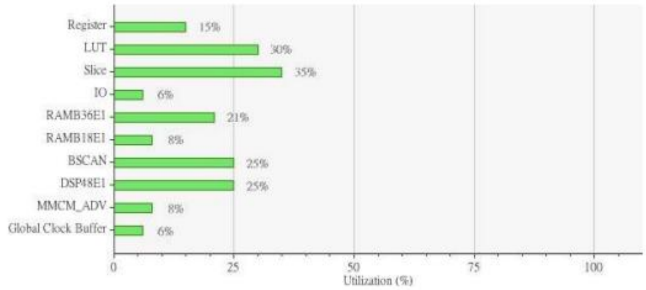

Figure 13. Implemented utilization.

IV. CONCLUSIONS

Wheezing detection systems have traditionally relied on desktop PCs, which are slow and lack portability. For home care, portable devices offer increased patient comfort. This study presents a portable WDSIP designed for PC-free wheezing analysis, suitable for remote medical applications. Implemented on a Xilinx FPGA, the WDSIP operates at 51.97 MHz, enabling rapid wheezing detection—a speed not attainable with conventional methods. Compatibility with the Xilinx PLB and control via the Xilinx MicroBlaze provide flexibility for integration with other biomedical signal systems within complex SoPCs. Furthermore, the WDSIP's implementation using advanced CMOS processes reduces power consumption, a key concern for PC-based systems used in long-term monitoring. Future improvements include hardware optimization to minimize resource usage and enhance commercial viability. Better management of noise interference and fixed-point computational errors is also necessary. Finally, the addition of peripheral devices, such as LCD displays or storage, would empower doctors to use the system for lung disease diagnosis and facilitate implementation in remote medical assistance scenarios.

REFERENCES

[1] Vital Signs. Available online: http://www.cdc.gov/ vitalsigns/Asthma/?s_cid=vitalsigns_063 (accessed on 30 December 2013).

[2] Global Surveillance, Prevention and Control of Chronic Respiratory Diseases: A Comprehensive Approach, 2007. Available online: http://www.who.int/gard/ publications/GARD%20Book%202007. pdf (accessed on 30 December 2013).

[3] Sovijarvi, A.R.A.; Malmberg, L.P.; Charbonneau, G.; Vanderschoot, J. Characteristics of breath sounds and adventitious respiratory sounds. Eur. Respir. Rev.2000, 77, 591–596.

[4] Karnath, B.; Boyars, M.C. Pulmonary auscultation. Hosp. Physician 2002, 38, 22–26.

[5] Quanjer, P.H.; Lebowitz, M.D.; Gregg, I.; Miller, M.R.; Pedersen, O.F. Peak expiratory flow: conclusions and recommendations of a working party of the european respiratory society. Eur. Respir. J. 1997, 24, S2–S8.